Non-equilibrium atomic simulation for Frenkel-Kontorova model with moving dislocation at finite temperature

Baiyili Liu(刘白伊郦), Shaoqiang Tang(唐少强)

Citation: Chin. Phys. B . 2020, 29(11): 110501 . **doi:** 10.1088/1674-1056/abaed4
Journal homepage: http://cpb.iphy.ac.cn; http://iopscience.iop.org/cpb

What follows is a list of articles you may be interested in

Evolution of the Internet AS-level topology:From nodes and edges to components

Xiao Liu(刘晓), Jinfa Wang(王进法), Wei Jing(景薇), Menno de Jong, Jeroen S Tummers, Hai Zhao(赵海)

Chin. Phys. B . 2018, 27(12): 120501 . **doi:** 10.1088/1674-1056/27/12/120501

Some new advance on the research of stochastic non-smooth systems

Wei Xu(徐伟), Liang Wang(王亮), Jinqian Feng(冯进钤), Yan Qiao(乔艳), Ping Han(韩平)

Chin. Phys. B . 2018, 27(11): 110503 . **doi:** 10.1088/1674-1056/27/11/110503

Detecting overlapping communities based on vital nodes in complex networks

Xingyuan Wang(王兴元), Yu Wang(王宇), Xiaomeng Qin(秦小蒙), Rui Li(李睿), Justine Eustace

Chin. Phys. B . 2018, 27(10): 100504 . **doi:** 10.1088/1674-1056/27/10/100504

Current loss of magnetically insulated coaxial diode with cathode negative ion

Dan-Ni Zhu(朱丹妮), Jun Zhang(张军), Hui-Huang Zhong(钟辉煌), Jing-Ming Gao(高景明), Zhen Bai(白珍)

Chin. Phys. B . 2018, 27(2): 020501 . **doi:** 10.1088/1674-1056/27/2/020501

Reduced one-body density matrix of Tonks–Girardeau gas at finite temperature

Fu Xiao-Chen, Hao Ya-Jiang

Chin. Phys. B . 2015, 24(9): 090501 . **doi:** 10.1088/1674-1056/24/9/090501

Non-equilibrium atomic simulation for Frenkel–Kontorova model with moving dislocation at finite temperature*

Baiyili Liu(刘白伊郦)[1] and Shaoqiang Tang(唐少强)[2,†]

[1] School of Physics and Electronic Engineering, Centre for Computational Sciences, Sichuan Normal University, Chengdu 610066, China
[2] HEDPS and LTCS, College of Engineering, Peking University, Beijing 100871, China

(Received 15 July 2020; revised manuscript received 4 August 2020; accepted manuscript online 13 August 2020)

We apply the heat jet approach to realize atomic simulations at finite temperature for a Frenkel–Kontorova chain with moving dislocation. This approach accurately and efficiently controls the system temperature by injecting thermal fluctuations into the system from its boundaries, without modifying the governing equations for the interior domain. This guarantees the dislocation propagating in the atomic chain without nonphysical damping or deformation. In contrast to the non-equilibrium Nosé–Hoover heat bath, the heat jet approach efficiently suppresses boundary reflections while the moving dislocation and interior waves pass across the boundary. The system automatically returns back to the equilibrium state after all non-thermal motions pass away. We further apply this approach to study the impact of periodic potential and temperature field on the velocity of moving dislocation.

Keywords: atomic simulation, finite temperature, moving dislocation, heat jet approach

PACS: 05.10.−a, 02.70.Ns, 61.72.Bb **DOI:** 10.1088/1674-1056/abaed4

1. Introduction

Atomic simulations have become instrumental for materials science and engineering at nano-scale or sub-micron scale. Simulating solids with moving dislocations at finite temperature is important for understanding the physical mechanism of interaction between heat and dislocation. It is known that the motion of dislocation is sensitively affected by thermal field.[1–3] In turn, the dislocations will influence the local thermal field and heat transport by interacting with phonon normal modes.[4–6] When mechanical behaviors are considered, technical difficulties arise and make finite temperature simulations a challenging task. One of the most difficult problems is to eliminate boundary reflections when a dislocation passes across the atomic interface. Another tough problem is to design an appropriate heat bath method to realize thermal-mechanical simulations at finite temperature.

In recent years, various artificial boundary conditions have been proposed to treat boundary reflections, such as variational boundary condition,[7,8] time history kernel boundary condition,[9–11] and perfectly matched layer.[12,13] They are mainly used in multiscale computations for thermal-mechanical problems. While these artificial boundary conditions efficiently damp out fine fluctuations of small amplitude, passing a dislocation across the atomic interface usually results in strong reflections. This comes from the strong local nonlinearity across the big jump in a dislocation profile. On the other hand, the perturbation on dislocations by temperature field generates many high-frequency waves, making the reflections more difficult to treat.

As the key point for finite temperature simulations, an appropriate heat bath should heat the lattice system accurately to the target temperature and preserve the dislocation profile without nonphysical deformation. Classical heat bath methods, such as Anderson heat bath,[14] Berendsen heat bath,[15] Nosé–Hoover heat bath,[16,17] and Langevin heat bath,[18] efficiently control the temperature by adjusting the momentum of each atom. These methods suit well thermal equilibrium problems, yet fail to simulate non-equilibrium problems with moving dislocation and other non-thermal motion.[19] As the appearance of dislocation leads to increment of system temperature, the excessive energy will be damped out by the dynamics of heat bath, leading to a wrongly damped moving dislocation.

In order to avoid the nonphysical deformation of moving dislocations, one may couple the heat bath with atomic boundary conditions.[20–22] For example, the non-equilibrium Nosé–Hoover heat bath method maintains the original lattice dynamics unchanged by connecting the thermostat with boundary atoms, thereby avoids the moving dislocation being wrongly deformed. It has been widely used to study heat transport[23–25] and thermal properties of lattice systems.[26–28] However, the non-equilibrium Nosé–Hoover heat bath usually adopts fixed or free boundary condition. It is effective only when the dislocation is away from the boundary. Reflections occur otherwise. Therefore, the atomic region has to be set big enough.

The heat bath and non-reflection boundary condition do not comply with each other in general. A heat bath produces

*Project supported by the National Natural Science Foundation of China (Grant Nos. 11890681, 11832001, and 11988102).
†Corresponding author. E-mail: maotang@pku.edu.cn

thermal energy and inputs it into the lattice system, whereas the non-reflection boundary condition damps out the inner energy by eliminating motions across the interface. To mitigate them, we developed an efficient thermostating technique for atomic simulations called as the heat jet approach. We verified that the approach accurately controls the temperature for one-dimensional harmonic chain[29] and two-dimensional lattices.[30,31] By a two-way boundary condition, we effectively inject the phonon heat source containing incoming normal modes into the atomic system, meanwhile allow interior waves freely propagating out.

In this work, we apply the heat jet approach to the one-dimensional Frenkel–Kontorova (F–K) model[32] to simulate a moving dislocation at finite temperature. Numerical simulations are performed, with comparison to the reference solution, and that by the non-equilibrium Nosé–Hoover heat bath method. We further study the impact of periodic potential and temperature on the velocity of moving dislocation.

2. Formulation and numerical method

We consider a monoatomic chain with pairwise F–K potential.[32] Each atom interacts with two adjacent atoms only. Motion of the system is governed by the Newton's law

$$m'\ddot{u}'_n = -\frac{\partial U(u')}{\partial u'_n} + f_{\text{ext}}. \tag{1}$$

Here, m' is the mass, and u'_n is the displacement of the n-th atom away from its equilibrium position. In simulations, we set the external force $f_{\text{ext}} = 0$. The F–K potential takes the form

$$U(u') = \sum_n \left[\frac{g'}{2}(u'_n - u'_{n-1})^2 + \frac{k'}{2}\left(1 - \cos(u'_n/a')\right)\right]. \tag{2}$$

Here, g' is the elastic constant, k' is the strength of the periodic potential, and a' is the lattice constant.

The governing equation of the F–K chain reads

$$m'\ddot{u}'_n = g'(u'_{n-1} - 2u'_n + u'_{n+1}) - k' \sin u'_n/a'. \tag{3}$$

To be specific, we choose aluminum mass $m' = 4.48 \times 10^{-26}$ kg and lattice constant $a' = 4.049$ Å as the characteristic mass and length. Considering atomic thermal vibration typically at picosecond,[33] we choose the characteristic time $t_c = 3 \times 10^{-13}$ s. With this choice, our dimensionless quantities are mostly scaled at the order of 1. As long as the real physical quantities are specified, other choice of t_c around picosecond also works, though the rescaled quantities will change their values accordingly.

According to the characteristic quantities, the dimensionless quantities are defined as follows:

$$a = 1, \quad u_n = u'_n/a', \quad t = t'/t_c, \tag{4}$$

$$g = g' t_c^2/m' = 1, \quad k = k'/g'a'. \tag{5}$$

The temperature is rescaled by $T_c = m'a'^2/k'_B t_c^2 = 5.91 \times 10^3$ K, where $k'_B = 1.38 \times 10^{-23}$ J/K is the Boltzmann constant. For the temperature $T = 0.0508$, the corresponding real temperature is $T' = T_c T = 300$ K.

After scaling, the dimensionless governing equation is written as

$$\ddot{u}_n = u_{n-1} - 2u_n + u_{n+1} - k \sin u_n. \tag{6}$$

For the sake of clarity, we present theoretical and numerical illustrations for the F–K chain with a single dislocation. The dislocation is represented by the following smoothed step function:

$$\begin{cases} u_j = 4 \arctan \beta(j), \\ \dot{u}_j = \dfrac{4\gamma\beta(j)}{\sqrt{1+\beta(j)^2}}, \end{cases} \tag{7}$$

with $\alpha = 0.9$, $\sigma = 0.05$, $\gamma = \sigma/\sqrt{1/\alpha^2 - 1}$, and $\beta(j) = \mathrm{e}^{-\sigma/\sqrt{1-\alpha^2}[2\pi(j-1-2N_0)]}$. The parameter N_0 represents the position of the dislocation. The jump across the dislocation is 2π, agreeing with the period of the potential.

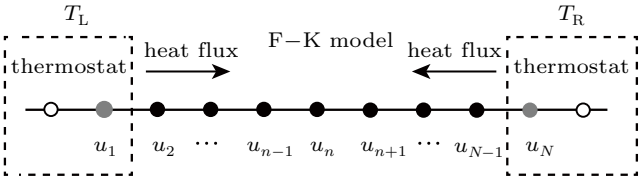

Fig. 1. The schematic of atomic simulation for the F–K chain.

To simulate a moving dislocation at finite temperature, we adopt the heat jet approach for heat bath.[29] Schematically shown in Fig. 1, it mainly consists of two parts: two-way boundary conditions and phonon heat sources. The two-way boundary conditions are composed of information of interior atoms and heat source term $f^{L(R)}(t)$, which are applied to the first atom and the last atom

$$\dot{u}_1 = -c_1\dot{u}_2 - \dot{u}_3 + c_2(u_1 - u_3) + f^L(t), \tag{8}$$

$$\dot{u}_N = -c_1\dot{u}_{N-1} - \dot{u}_{N-2} + c_2(u_N - u_{N-2}) + f^R(t). \tag{9}$$

The phonon heat sources are injected by the two-way boundary conditions, without modifying the governing equations for the interior domain. This guarantees the moving dislocation not to be wrongly damped. The heat sources take phonon representations superposed by incoming waves

$$f^L(t) = \dot{w}_1 + c_1\dot{w}_2 + \dot{w}_3 - c_2(w_1 - w_3), \tag{10}$$

$$f^R(t) = \dot{v}_1 + c_1\dot{v}_2 + \dot{v}_3 - c_2(v_1 - v_3), \tag{11}$$

$$w_j = \sum_p \sqrt{\frac{T}{N_c\omega_p^2}} \cos\left(\omega_p t - \xi_p \cdot j + \varphi_p^L\right), \quad j = 1,2,3, \tag{12}$$

$$v_j = \sum_p \sqrt{\frac{T}{N_c\omega_p^2}} \cos\left(\omega_p t + \xi_p \cdot j + \varphi_p^R\right), \quad j = N-2, N-1, N. \tag{13}$$

Here, the coefficients $c_1 = 2+2\sqrt{2}$ and $c_2 = 2+\sqrt{2}$. For a chain with N atoms, $\xi_p = 2\pi p/N$ is the wave number, $\omega_p = 2\sin\xi_p/2$ is the normal mode frequency, p is an integer, and N_c is the total number of normal modes. The phases $\varphi_p^{L(R)}$ are randomly chosen in the interval $[0, 2\pi]$.

The wave number of the phonon representations is within $[0,\pi]$ in theory. However, it needs to be truncated in practical simulations for two reasons. On the one hand, the long waves $\xi \to 0$ need a much longer atomic chain to resolve. On the other hand, the short waves $\xi \to \pi$ move slowly, hence need a much longer time to pass across the whole chain. In our study of moving dislocation, we only simulate a short chain for a computing time on the order of 10^3. To be precise, we need truncate the wave number band to $[\pi/8, 7\pi/8]$, which is broad enough for describing the thermal field and adequate for studying the relationship between the moving dislocation and the thermal field.

For time integration of the Newton's equation, we use the velocity verlet scheme with a time step $\Delta t = 0.01$. The velocity verlet scheme is an energy-conserved symplectic algorithm,[34,35] which is indispensable for long-time atomic simulations. We have verified that the second order Runge–Kutta method may exhibit instability for long time simulations of a harmonic chain with the Nosé–Hoover heat bath.[36] The velocity verlet algorithm for the n-th atom at the time step l reads

$$\dot{u}_n^{l+\frac{1}{2}} = \dot{u}_n^l + \frac{\Delta t}{2} F_n^l, \quad n = 2,3,\ldots,N-1, \tag{14}$$

$$u_n^{l+1} = u_n^l + \Delta t \dot{u}_n^l + \frac{\Delta t^2}{2} F_n^l, \tag{15}$$

$$\dot{u}_n^{l+1} = \dot{u}_n^{l+\frac{1}{2}} + \frac{\Delta t}{2} F_n^{l+1}. \tag{16}$$

The boundary atom motions are integrated by the following scheme, with the left one as an example,

$$\dot{u}_1^{l+\frac{1}{2}} = -c_1 \dot{u}_2^{l+\frac{1}{2}} - \dot{u}_3^{l+\frac{1}{2}} + c_2(u_3^l - u_1^l) + f_L^l, \tag{17}$$

$$u_1^{l+1} = u_1^l + \Delta t \dot{u}_1^{l+\frac{1}{2}}, \tag{18}$$

$$\dot{u}_1^{l+1} = -c_1 \dot{u}_2^{l+1} - \dot{u}_3^{l+1} + c_2(u_3^{l+1} - u_1^{l+1}) + f_L^{l+1}. \tag{19}$$

In all computations, we simulate the F–K chain with $N = 512$ atoms. The wave number $\xi_p = 2\pi p/N$ within $[\pi/8, 7\pi/8]$ leads to the integer p ranging from $N/16$ to $7N/16$, resulting in the total number of normal modes $N_c = 3N/8 + 1 = 193$. Unless otherwise specified, we take the target temperature $T = 0.0508$ (300 K) and the coefficient $k = 0.1$.

3. Numerical results

First, we simulate a moving dislocation in the F–K chain by the heat jet approach and make comparison with reference solution which is obtained from a long enough chain without any reflection. To better examine the influence of boundary conditions, we simulate the dislocation at $T = 0$ to avoid the effects of thermal field. From Figs. 2(a)–2(c), it can be seen that the dislocation propagates toward the right boundary without any numerical artifact. The front of dislocation invokes some waves moving fast to both sides. In Fig. 2(d), the dislocation has freely passed away from the atomic region. Numerical reflections are about 1%–2%. During the dislocation moving inside the atomic region, the numerical solution of the heat jet approach agrees well with the reference solution. This manifests that the two-way boundary condition well suppresses reflections for out-going waves.

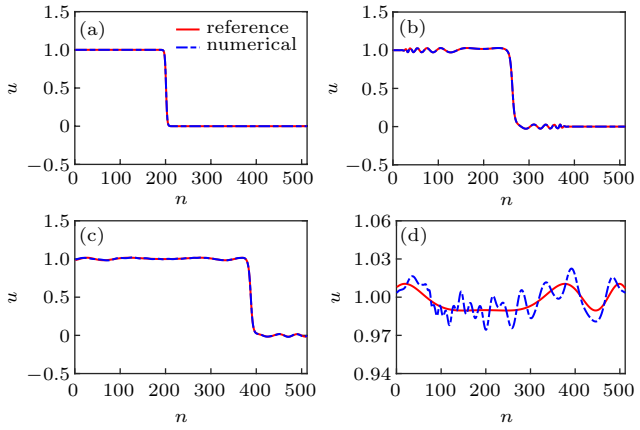

Fig. 2. Dislocation propagation in the F–K chain at $T = 0$: (a) $t = 0$; (b) $t = 200$; (c) $t = 600$; (d) $t = 1500$. The displacement u_n is rescaled by 2π. In following figures, u_n is rescaled in the same way.

Then, we simulate a moving dislocation at temperature $T = 0.0508$ (300 K), and make comparison with the non-equilibrium Nosé–Hoover heat bath.[20] The F–K chain is firstly heated to the equilibrium state, then a dislocation profile is superimposed to the displacement and velocity. For the heat jet approach in Fig. 3(a), the dislocation with small thermal fluctuations propagates toward the right boundary and then freely passes out of the atomic region. No reflected dislocation or other artifacts appear at the boundary. However, for the non-equilibrium Nosé–Hoover heat bath in Fig. 3(b), the dislocation is reflected by the fixed boundary conditions and can not escape from the atomic region.

High temperature leads to strong nonlinearity, making it more difficult to control the temperature and to eliminate the boundary reflections. To test whether the heat jet approach endures under high temperature, we simulate a moving dislocation at temperature $T = 0.1354$ (800 K). From Fig. 4(a), we observe that the displacement profile is similar to that at 300 K, showing the effectiveness of the heat jet approach at high temperature. The difference between low temperature and high temperature lies in thermal fluctuation amplitudes. The corresponding system temperature $T(t) = \sum_{n=1}^{N} \dot{u}_n^2(t)/N$ is shown in Fig. 4(b). The system temperature rises up quickly and keeps fluctuating around the equilibrium temperature. At time $t = 1\times10^4$, the system temperature increases due to the super-

imposed dislocation. Then it quickly reduces to the target temperature after the dislocation passing out of the atomic region. This test illustrates that the heat jet approach efficiently controls the temperature and suppresses spurious reflections even at high temperature. The system automatically returns back to the equilibrium state after all non-thermal motions pass away.

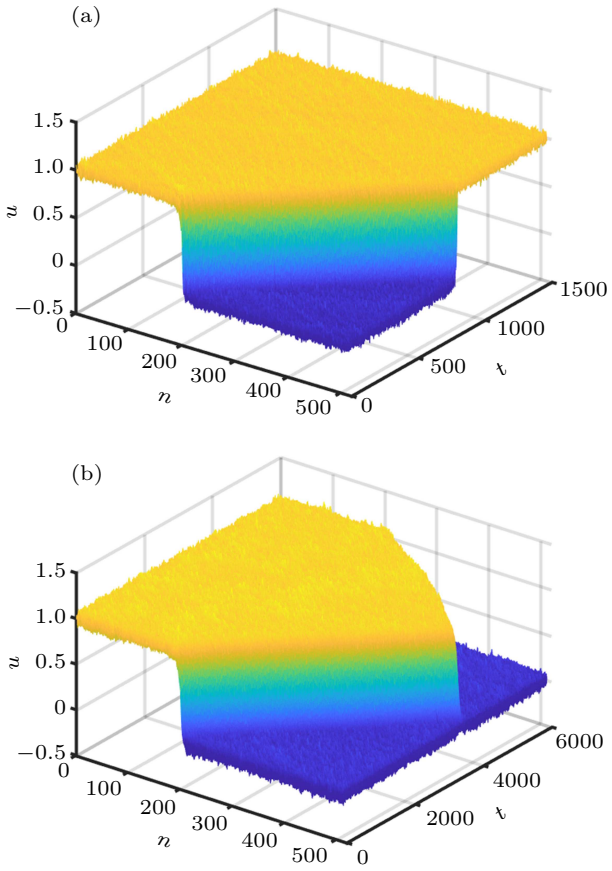

Fig. 3. Dislocation propagation in the F–K chain at temperature $T = 0.0508$ (300 K) thermostated by (a) heat jet approach; (b) non-equilibrium Nosé–Hoover heat bath.

The velocity of a moving dislocation in the F–K chain is sensitively affected by the elastic coefficient k and the temperature field. To find out the relationship between the velocity and coefficient k, we simulate a moving dislocation under coefficients $k = 0.05, 0.1, 0.5$ at temperature $T = 0$. As shown in Fig. 5(a), each point represents the position of the dislocation at different time. The slope of the interpolated line is the velocity of the moving dislocation. It increases for smaller k. This may be explained with the group velocity of the F–K model. For $T = 0$ or low temperature, the periodic potential $\sin u_n$ can be approximate by u_n as $|u_n| \ll 1$. Thus the governing equation is approximated by

$$\ddot{u}_n = u_{n-1} - 2u_n + u_{n+1} - ku_n. \tag{20}$$

Substituting a monochromatic wave $u_n(t) \sim \mathrm{e}^{\mathrm{i}(\omega t + \xi n)}$ into it, we obtain the dispersion relation

$$\omega = \sqrt{4\sin^2\frac{\xi}{2} + k}. \tag{21}$$

Accordingly, the group velocity at wave number ξ is

$$\frac{\mathrm{d}\omega}{\mathrm{d}\xi} = \frac{\sin\xi}{\sqrt{4\sin^2\frac{\xi}{2} + k}}. \tag{22}$$

It is plotted in Fig. 5(b). For a fixed wave number ξ, the group velocity decreases when k increases. It is worth noting that the condition $|u_n| \ll 1$ is not satisfied for high temperature.

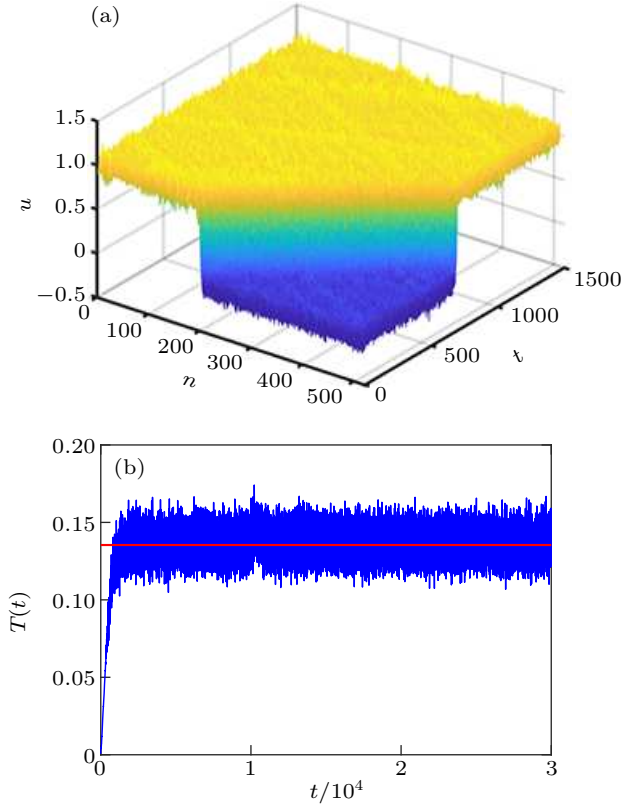

Fig. 4. Dislocation propagation in the F–K chain at temperature $T = 0.1354$ (800 K) thermostated by the heat jet approach: (a) the displacement profile of the moving dislocation; (b) the system temperature.

When the thermal field is taken into account, the motion becomes more complicated. As thermal fluctuations are superposed by normal modes with various wave numbers and random phases, temperature is not the only factor that determines the velocity of the moving dislocation. Through numerical simulations, we find that the velocity does not always increase along with temperature. As shown in Fig. 6, the velocity at $T = 0.0846$ (500 K) is smaller than that at $T = 0$ and $T = 0.0508$ (300 K). There is no monotonous relationship between the velocity and temperature. Besides, the velocity appears different for each run even at the same temperature, due to the random phases in thermal fluctuations. This phenomenon is also observed in dislocation simulations with the non-equilibrium Nosé–Hoover heat bath. We speculate that the velocity of a moving dislocation relies on the frequency, phase, and amplitude of the normal modes. It demands further study to better understand the relationship between the velocity and normal modes in the F–K model.

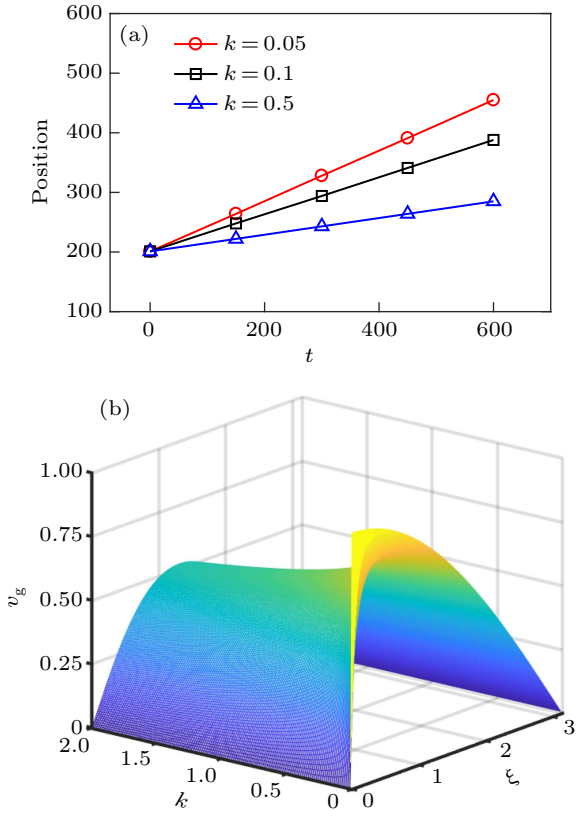

Fig. 5. (a) The position of the dislocation at temperature $T = 0$ with $k = 0.07, 0.1, 0.5$; (b) the group velocity of the F–K chain.

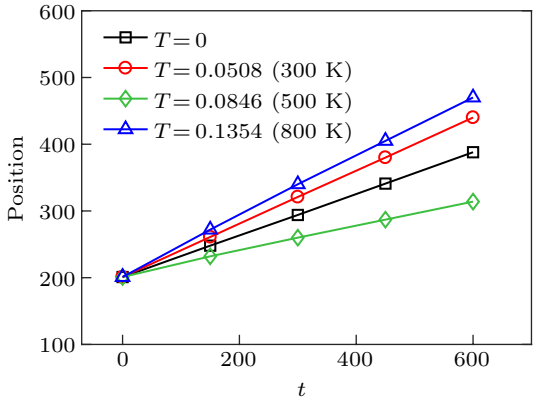

Fig. 6. The position of the front of the dislocation in the F–K chain with $k = 0.1$ under different temperature.

4. Conclusion

In summary, we successfully apply the heat jet approach to realize moving dislocation simulations in the F–K chain at finite temperature. By this approach, we heat the system accurately to the equilibrium temperature through injecting thermal fluctuations into the atomic region under the two-way boundary conditions. Thermostating at boundaries guarantees the internal governing equations unchanged, and maintains the dislocation propagating inside the atomic chain without non-physical damping or deformation. Comparing with the reference solution and the non-equilibrium Nosé–Hoover heat bath, this approach efficiently eliminates boundary reflections when the dislocation passes across the boundary. The system automatically returns back to the equilibrium state after all non-thermal motions pass away. Furthermore, we have investigated the impact of periodic potential and temperature field on the velocity of moving dislocation. In view of its accurate temperature control and efficient reflection suppression, the heat jet approach may be incorporated together with many existing multiscale methods to study thermal-mechanical problems at finite temperature.

Acknowledgments

We would like to thank Dr. Xuewei Xia for careful reading of the manuscript and express gratitude to Prof. Hong Guo for useful discussions.

References

[1] De Hosson J T M, Roos A and Metselaar E D 2001 *Philos. Mag. A* **81** 1099
[2] Olmsted D L, Hector Jr L G, Curtin W A, *et al.* 2005 *Modell. Simul. Mater. Sci. Eng.* **13** 371
[3] Gurrutxaga-Lerma B 2017 *Int. J. Solids Struct.* **108** 263
[4] Al-Ghalith J, Ni Y and Dumitrică T 2016 *Phys. Chem. Chem. Phys.* **18** 9888
[5] Ni Y, Xiong S, Volz S, *et al.* 2014 *Phys. Rev. Lett.* **113** 124301
[6] Chen Z, Ge B, Li W, *et al.* 2017 *Nat. Commun.* **8** 1
[7] E W, Engquist B, Li X, *et al.* 2007 *Commun. Comput. Phys.* **2** 367
[8] Li X and E W 2007 *Phys. Rev. B* **76** 104107
[9] Liu W K, Karpov E G and Park H S 2006 *Nano mechanics and materials: theory, multiscale methods and applications* (John Wiley & Sons)
[10] Farrell D E, Karpov E G and Liu W K 2007 *Comput. Mech.* **40** 965
[11] Tang S Q, Liu W K, Karpov E G, *et al.* 2007 *Chin. Phys. Lett.* **24** 161
[12] To A C and Li S 2005 *Phys. Rev. B* **72** 035414
[13] Li S, Liu X, Agrawal A, *et al.* 2006 *Phys. Rev. B* **74** 045418
[14] Andersen H C 1980 *J. Chem. Phys.* **72** 2384
[15] Berendsen H J C, Postma J P M, van Gunsteren W F, *et al.* 1984 *J. Chem. Phys.* **81** 3684
[16] Nosé S 1984 *J. Chem. Phys.* **81** 511
[17] Hoover W G 1985 *Phys. Rev. A.* **31** 1695
[18] Bussi G and Parrinello M 2007 *Phys. Rev. E.* **75** 056707
[19] Li S, Sheng N and Liu X 2008 *Chem. Phys. Lett.* **451** 293
[20] Lepri S, Livi R and Politi A 2003 *Phys. Rep.* **377** 1
[21] Karpov E G, Park H S and Liu W K 2007 *Int. J. Numer. Eng.* **70** 351
[22] Dhar A and Dandekar R 2015 *Physica A* **418** 49
[23] Hu G and Cao B 2014 *Chin. Phys. B* **23** 096501
[24] Zhong Y, Zhang Y, Wang J, *et al.* 2013 *Chin. Phys. B* **22** 070505
[25] Zhang C, Kang W and Wang J 2016 *Phys. Rev. E.* **94** 052131
[26] Li B, Wang L and Casati G 2004 *Phys. Rev. Lett.* **93** 184301
[27] Ai B and Hu B 2011 *Phys. Rev. E* **83** 011131
[28] Rurali R, Cartoixà X and Colombo L 2014 *Phys. Rev. B* **90** 041408
[29] Tang S and Liu B 2015 *Comm. Comput. Phys.* **18** 1445
[30] Liu B and Tang S 2016 *Coupled Syst. Mech.* **5** 371
[31] Liu B, Tang S and Chen J 2017 *Comput. Mech.* **59** 843
[32] Braun O M and Kivshar Y S 2013 *The Frenkel-Kontorova model: concepts, methods, and applications* (Springer Science & Business Media)
[33] Cao G, Chen X and Kysar J W 2006 *J. Mech. Phys. Solids* **54** 1206
[34] Ruth R D 1983 *IEEE Trans. Nucl. Sci.* **30** 2669
[35] Feng K 1986 *J. Comput. Math.* **4** 279
[36] Liu B and Tang S 2017 *Phys. Rev. E* **96** 013308